Electrochemistry Communications 150 (2023) 107488

Contents lists available at ScienceDirect

Electrochemistry Communications

journal homepage: www.elsevier.com/locate/elecom

Sodium-ion diffusion coefficients in tin phosphide determined with advanced electrochemical techniques

Jun Wang [a], Emmanuel Pameté [b], Shengli Yan [a], Wenhua Zhao [a,*], Jianhui Zhang [a,*], Xiaotong He [a], Zhazira Supiyeva [c], Qamar Abbas [d,e,*], Xuexue Pan [a,d,*]

[a] Zhongshan Polytechnic, Zhongshan 528404, China
[b] INM - Leibniz Institute for New Materials, Campus D2 2, 66123 Saarbrücken, Germany
[c] Al-Farabi Kazakh National University, 71 al-Farabi Ave., 050040 Almaty, Kazakhstan
[d] Institute of Chemistry and Technical Electrochemistry, Faculty of Chemical Technology, Poznan University of Technology, Berdychowo 4, 60-965 Poznan, Poland
[e] Institute for Chemistry and Technology of Materials, Graz University of Technology, Stremayrgasse 9, 8010 Graz, Austria

ARTICLE INFO

Keywords:
Tin phosphide
Na^+ diffusion coefficients
Galvanostatic/potentiostatic intermittent titration technique
Electrochemical impedance spectroscopy

ABSTRACT

Sodium ion insertion plays a critical role in developing robust sodium-ion technologies (batteries and hybrid supercapacitors). Diffusion coefficient values of sodium (D_{Na+}) in tin phosphide between 0.1 V and 2.0 V vs. Na/Na^+ are systematically determined by galvanostatic intermittent titration technique (GITT), electrochemical impedance spectroscopy (EIS), and potentiostatic intermittent titration technique (PITT). These values range between 4.55×10^{-12} cm^2 s^{-1} and 1.94×10^{-8} cm^2 s^{-1} and depend on the insertion/de-insertion current and the thickness of the electrode materials. Additionally, D_{Na+} values differ between the first and second cation insertion because of the solid electrolyte interface (SEI) formation. D_{Na+} vs. insertion potential alters non-linearly in a "W" form due to the strong interactions of Na^+ with tin phosphide particles. The results reveal that GITT is a more appropriate electrochemical technique than PITT and EIS for evaluating D_{Na+} in tin phosphide.

1. Introduction

With a growing concern about fossil fuels depletion and the environmental impact of energy production from fuels, demands for energy storage systems are rapidly increasing [1]. One type of the latter is Li-ion capacitors (LICs) which consist of an electric double-layer (EDL) positive electrode and a lithiated battery-type anode capable of reversible insertion/de-insertion of lithium cations and storing high amounts of energy (greater than 100 Wh kg^{-1}) [2]. Owing to the inexpensive nature of sodium and its abundant distribution, Na-ion capacitors (NICs) are being developed to replace LICs [3]. This transition also allows replacing Cu current collectors with cost-effective aluminum ones in sodium-ion systems [4]. Since lithium is prone to alloy formation with aluminum at low potentials, replacing the former with sodium can also solve the problem of alloying [5]. Tin phosphide is an extensively explored electrode material due to its theoretical capacity of 1132 mAh g^{-1} and a range of cations (Li^+, Na^+, and K^+) storage properties. It is considered an option for the anodic material for NIBs and NICs [6]. The Na^+ diffusion coefficient (D_{Na+}) in tin phosphide limits the high power capability (or rate capability) of the resulting device. Therefore, understanding the transport properties of Na^+ in tin phosphide is essential for improved energy storage and delivery. Thus, it is crucial to identify simple methods to evaluate the kinetic behavior of tin phosphide, of which D_{Na+} is a critical parameter.

This work aims to implement GITT, PITT, and EIS methods to evaluate D_{Na+} in tin phosphide. First, D_{Na+} in tin phosphide is studied using the well-known GITT during the initial three cycles. Then, D_{Na+} is compared with different electrode thicknesses, and the effect of specific currents on the insertion/de-insertion of sodium ions is determined. Finally, two electrochemical analysis methods PITT and EIS are introduced to compare D_{Na+} values with the GITT technique.

2. Experimental

2.1. Fabrication of tin phosphide electrodes

Tin phosphide powder was prepared by grinding together 5 g tin and 1 g red phosphorous for 4 h with the help of 18 tungsten carbide balls (Ø = 10 mm) under Ar in a high-energy planetary ball mill. Electrode material containing 85 mass% tin phosphide, 7 mass% C-NERGY SUPER

* Corresponding authors.
E-mail addresses: zhaowenhua@zspt.edu.cn (W. Zhao), jianhuizh@zspt.edu.cn (J. Zhang), qamar.abbas@tugraz.at (Q. Abbas), panxuexue@zspt.edu.cn (X. Pan).

https://doi.org/10.1016/j.elecom.2023.107488
Received 1 January 2023; Received in revised form 4 April 2023; Accepted 5 April 2023
Available online 18 April 2023
1388-2481/© 2023 The Author(s). Published by Elsevier B.V. This is an open access article under the CC BY license (http://creativecommons.org/licenses/by/4.0/).

C65 conductive carbon black, and 8 mass% carboxymethyl cellulose sodium salt (mixed in deionized water with a magneton and stirring for 3 h) and coated onto a copper foil. The coatings were dried under a vacuum at 120 °C overnight.

2.2. GITT, PITT, and EIS for tin phosphide electrodes

Sodium inserted in tin phosphide working electrodes was examined in 2025-type coin cells vs. a Na counter/reference electrode with a Whatman GF/D separator in 1 mol L^{-1} $NaClO_4$ in EC:PC (1:1 by volume). GITT, EIS, and PITT investigations on tin phosphide electrodes were executed with a LANDT battery test system (CT3002A) and a VSP electrochemical workstation from BioLogic.

For GITT, cells were discharged/charged at 50 mA g^{-1} (per mass of tin phosphide) for 30 min, then relaxed for 30 min at open circuit potential. The step continued until the cut-off potential of 10 mV or 2.0 V vs. Na/Na^+. When GITT was performed at 250 mA g^{-1}, pulse time was reduced to 5 min. D_{Na+} of tin phosphide from GITT curves was computed from Eq. (1) [7,8].

$$D_{GITT} = \frac{4L^2}{\prod\tau}\left(\frac{\Delta E_s}{\Delta E_t}\right)^2 .\tau << \frac{L^2}{D_{GITT}} \quad (1)$$

where τ represents the current pulse (30 min); L is denoted as electrode thickness; ΔE_s or ΔE_t (without IR drop) is defined as potential change during a steady pulse or constant current pulse.

A 10 mV potential stage for the PITT experiment was stepped during discharging between 0.3 V and 10 mV vs. Na/Na^+ and charging from 10 mV and 0.9 V vs. Na/Na^+. Each 10 mV potential was kept until reaching 5 mA g^{-1}. D_{Na+} of tin phosphide from PITT curves was calculated using Eq. (2) [9].

$$D_{PITT} = \left(\frac{\Delta \text{In I(t)}}{\Delta t}\right)\frac{4(L)^2}{\prod^2}.t >> \frac{L^2}{D_{PITT}} \quad (2)$$

where $I(t)$ represents the current measured during a constant potential step.

For EIS experiments, the cell was examined after 30 min discharge/charge at 50 mA g^{-1} and 30 min rest. EIS measurements were recorded after 30 min rest with a potential amplitude of 10 mV and a frequency range from 100 kHz to 1 mHz. D_{Na+} of tin phosphide from EIS curves was assessed based on Eq. (3) [7,10].

$$D_{EIS} = \frac{1}{2}\left[\frac{V_M}{AF\sigma_W}\frac{\Delta E}{\Delta x}\right]^2 \quad (3)$$

where V_M is defined as the molar volume of tin phosphide; A refers to the electrode/electrolyte contact area; F stands for the Faraday constant (96,486C mol^{-1}), and σ_W is expressed as Warburg coefficient obtained from the slope of Z' vs. $\omega^{-1/2}$ plots (ω is the angular frequency). $\Delta E/\Delta x$ is denoted as the slope of potential vs. Na^+ concentration x.

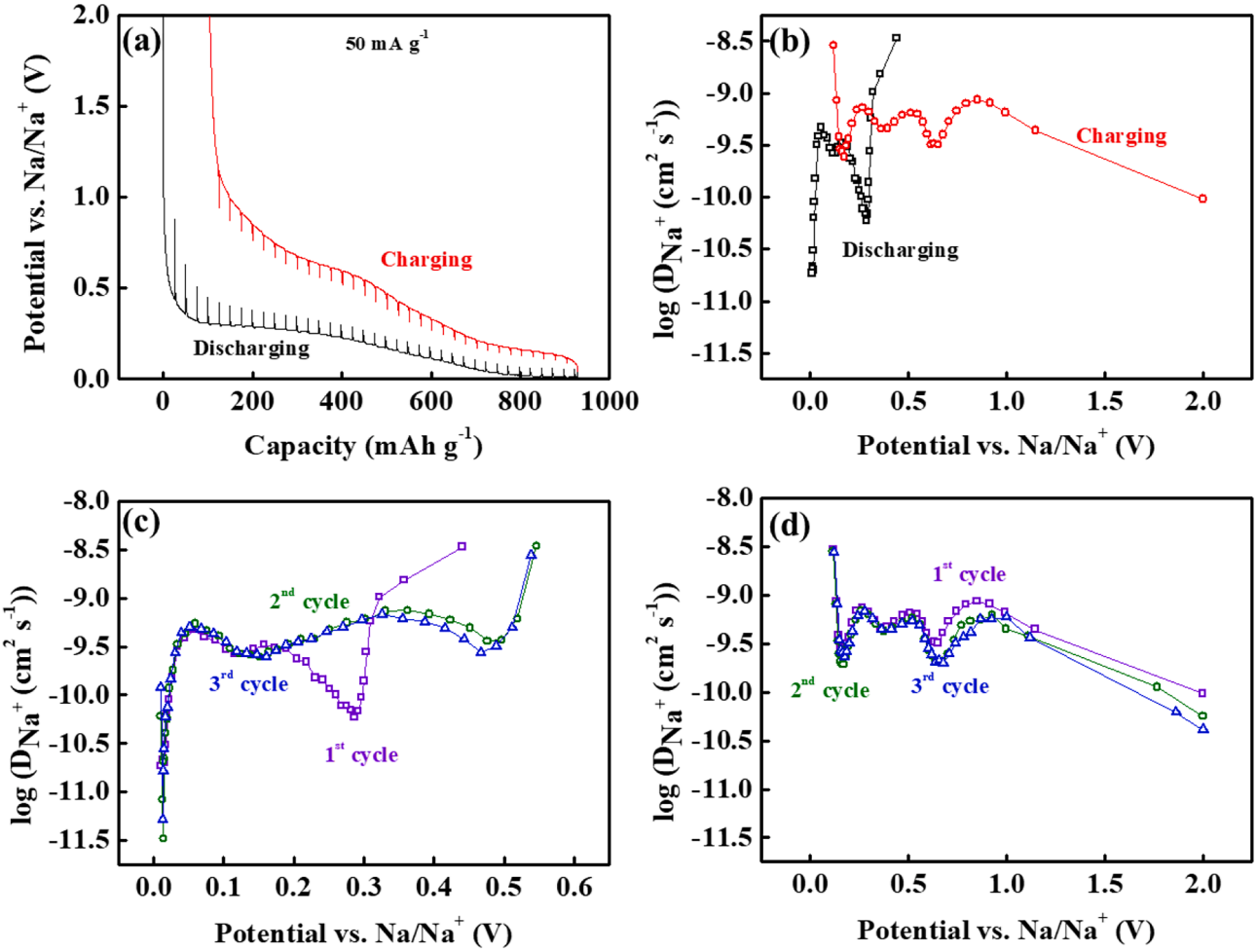

Fig. 1. (a) The GITT curves of tin phosphide electrode with a selected thickness of 30 μm at 50 mA g^{-1} during the first cycle in the potential range of 10 mV to 2.0 V vs. Na/Na^+. (b) D_{Na+} computed from GITT curves for tin phosphide electrode during the first cycle at 50 mA g^{-1}. D_{Na+} is calculated from the first, second, and third (c) discharge and (d) charge GITT curves for the tin phosphide electrode at 50 mA g^{-1}.

3. Results and discussion

3.1. D_{Na+} in tin phosphide electrode at different cycles by GITT

Owing to its ease of use in analyzing the entire range of sodium insertion, GITT was first introduced to evaluate D_{Na+} of tin phosphide electrodes. As shown in Fig. 1a, the reversible capacity is 824 mAh g^{-1} (initial capacity of 928 mAh g^{-1} minus irreversible value of 104 mAh g^{-1}) at a cut-off potential of 10 mV vs. Na/Na^+. The log(D_{Na+}) vs. potential plots in Fig. 1b shows three minima in both the discharging and charging processes related to the two plateaus and a slope range of the charge–discharge curve. In the discharge process, D_{Na+} ranges from 3.34×10^{-9} cm^2 s^{-1} to 1.84×10^{-11} cm^2 s^{-1}. In the charging process, D_{Na+} is distributed in a narrow range from 2.88×10^{-9} cm^2 s^{-1} to 9.57×10^{-11} cm^2 s^{-1}. The second and third cycles are shown in *Supporting Information*, Fig. S1a-b. The third minimum of D_{Na+} is always lower during discharging periods. This is attributed to the significant volume expansion and the pulverization of tin phosphide particles during further sodium insertion at low potential.

The obtained D_{Na+} values in the second and third cycles are identical, as shown in Fig. 1c-d. This finding illustrates that repeating cycles does not affect D_{Na+}. However, D_{Na+} from the discharge curves in the first cycle differs from the second and third cycles. When the insertion potential is higher than 0.3 V vs. Na/Na^+, D_{Na+} in the first discharge part is superior to that in the second cycle because of the formation of the SEI. Additionally, D_{Na+} in the first discharge curve shows the initial decrease and then increases from 0.3 V to 0.2 V vs. Na/Na^+, which is still lower than the values in the second cycle. This behavior suggests that Na^+ is initially inserted into tin phosphide particles, which results from high kinetic barriers in the plateau region.

3.2. Influence of electrode thickness on D_{Na+} in tin phosphide

D_{Na+} in tin phosphide with the different thicknesses of 30 μm, 45 μm, and 60 μm were determined by GITT and shown in Fig. 2a-b. Here, sodium insertion in tin phosphide occurred at 10 mV vs. Na/Na^+, yielding a value of 928 mAh g^{-1} (Fig. 1a), 880 mAh g^{-1} and 782 mAh g^{-1} (*Supporting Information*, Fig. S2a and S2c) for the thinner, medium and thicker electrodes, respectively. The decreased capacity value is due to the enhanced resistance of coated film on the Cu foil. According to the internal resistance (R) formula of electrode material , .

$$R = \rho \frac{L}{S} \tag{4}$$

where ρ and L are the resistivity and thickness of the electrodes, respectively, and S is the surface area of the electrode. When the thickness of the film coated on the electrode increases, the internal resistance of the electrode increases, resulting in capacity reduction [11]. D_{Na+} of coated tin phosphide film with 60 μm in the first cycle is almost three times higher than with 30 μm. This is slightly different from the theoretical result according to formula (1). When the thickness is doubled, D_{Na+} should be increased by four times. Due to the facile stacking nature of Sn_4P_3 nanoparticles during the coating process, sodium ion flux will be considerably blocked, which further contributes to

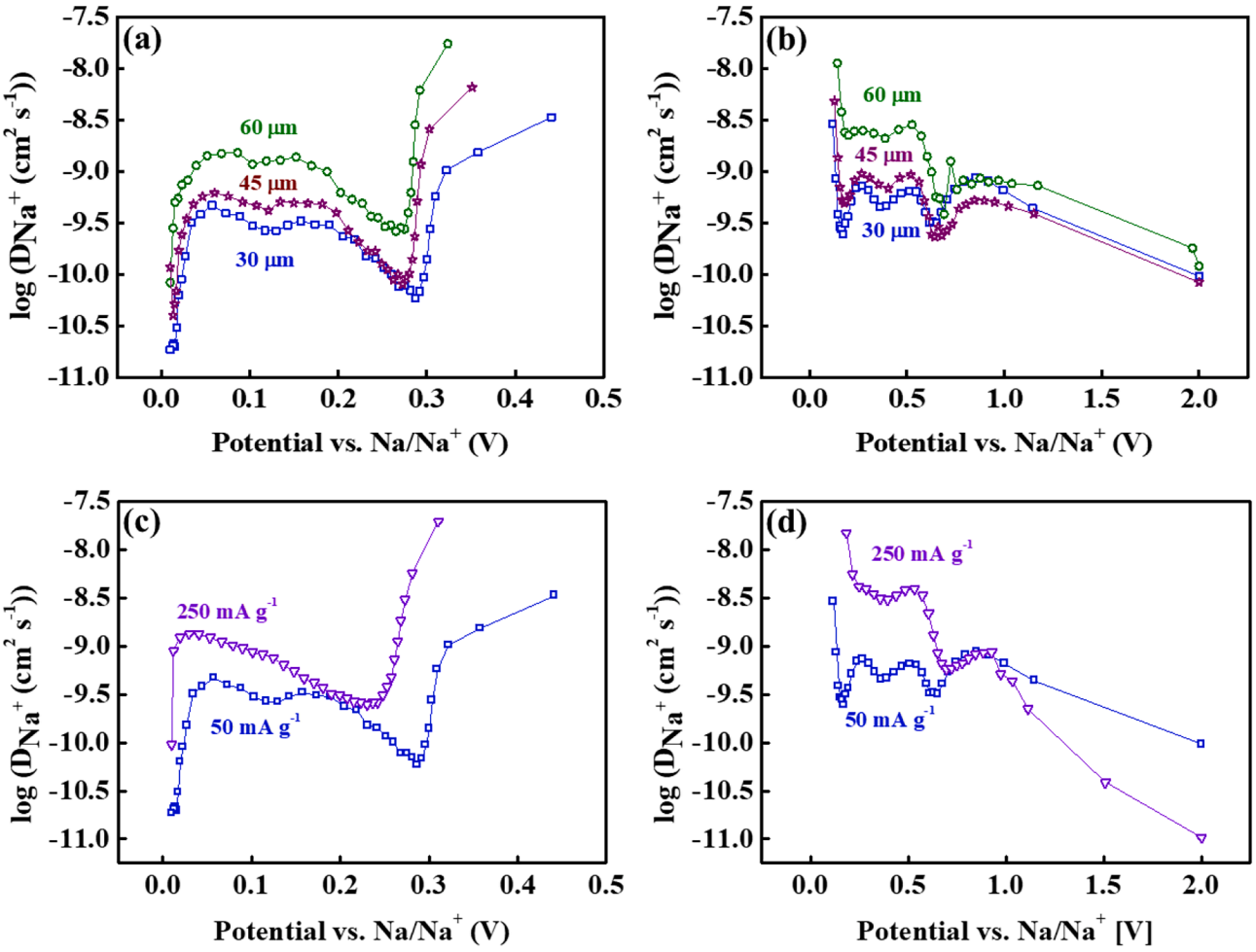

Fig. 2. D_{Na+} computed from the first (a) discharge and (b) charge GITT curves from a thickness of 30 μm, 45 μm and 60 μm electrodes at 50 mA g^{-1}. D_{Na+} calculated from the first (c) discharge and (d) charge GITT curves for a thickness of 30 μm electrode at 50 mA g^{-1} and 250 mA g^{-1}.

high-concentration polarization. Also, the stacking issue interrupts the even distribution of active materials in the conductive matrix, creating an additional adverse impact on the electrical percolation of the entire electrode [12]. D_{Na+} of electrode thickness with 45 μm is between 60 μm and 30 μm. All samples show similar variations; however, there are differences between the bare and Na-doped samples. The difference between the charge and discharge plateau of the 30 μm and 45 μm electrodes is lower than that of the 60 μm electrode due to the serious potential hysteresis in the thick electrode.

3.3. Influence of insertion/de-insertion current on the D_{Na+} of tin phosphide

Na^+ insertion into tin phosphide is performed at two specific current values (50 mA g^{-1} and 250 mAh g^{-1}) with the first sodiated capacities of 928 mAh g^{-1} (Fig. 1a) and 656 mAh g^{-1} (Fig. S3a), respectively. The first insertion plateau decreases from 0.30 V vs. Na/Na^+ to 0.26 V vs. Na/Na^+ by increasing the current. D_{Na+} upshifts three times after the increased current, except for the de-insertion potential of 0.6 V vs. Na/Na^+. D_{Na+} values of tin phosphide electrode at 250 mAh g^{-1} are in the range of 1.94×10^{-8} cm^2 s^{-1} to 9.54×10^{-11} cm^2 s^{-1} during discharge as shown in Fig. 2c. In contrast, those of tin phosphide electrode range from 1.47×10^{-8} cm^2 s^{-1} to 1.03×10^{-11} cm^2 s^{-1} during charging (Fig. 2d). Compared to D_{Na+} values at 50 mAh g^{-1}, the increase of the D_{Na+} values is caused by the insertion process, which cannot proceed completely at a higher specific current because the bulk of tin phosphide material is not fully accessible. Two minima of the obtained D_{Na+} values are seen for the tin phosphide electrode at 0.50–0.55 V and 0.35–0.40 V vs. Na/Na^+ associated with two long quasi-plateaus in the potential vs. capacity plot. The absence of minima from 0.06 V to 0.16 V vs. Na/Na^+ suggests that the phase transitions cause a rapid decrease in D_{Na+}. Fig. S4a and S4c show that when the electrode is charged and discharged for the second time with high currents of 150 mA g^{-1} and 250 mA g^{-1}, the distance between the charge and discharge plateau gradually widens compared with Fig. S1a. Nevertheless, D_{Na+} increases when increasing the applied current and the values for 150 mA g^{-1} are closer to those for 250 mA g^{-1} and much higher than 50 mA g^{-1} (Fig. S4e) due to the limitation of volume expansion in the former case. Notably, at higher potential from 1.0 V to 2.0 V vs. Na/Na^+ at 250 mA g^{-1} does not change smoothly compared with 150 mA g^{-1} and 50 mA g^{-1} (Fig. S4f) due to the possible structural deformation of Sn_4P_3. According to the literature, addition of a buffer to Sn_4P_3 could solve this issue [13–15].

3.4. ESR, R_{ct}, and EDR of tin phosphide electrodes by EIS

EIS measures ESR, R_{ct}, and EDR values during sodium insertion. The potential curves of the tin phosphide electrode with a thickness of 30 μm during the EIS experiment are presented in *Supporting Information*, Fig. S5a. The results show a reversible capacity of 679 mAh g^{-1} and an irreversible capacity value of 77 mAh g^{-1}, which are lower than the values measured in the GITT curve. This is because the EIS measurements were conducted only after a rest period. Nyquist plots with three typical regions under different discharge/charge states for tin phosphide electrodes are shown in *Supporting Information*, Fig. S5b-c. ESR and R_{ct} values increase, respectively, from 10.3 Ω to 10.8 Ω and from 67.5 Ω to 98.7 Ω, as shown in Fig. 3a and *Supporting Information*, Fig. S5d. This increase is related to the formation of SEI during the first discharge performed at 50 mA g^{-1}. The resistance values gradually decrease to 8.7 Ω (ESR) and 68.4 Ω (CTR) at the vertex potential of 10 mV vs. Na/Na^+ due to the creation of sodiated tin phosphide to improve the conductivity of the electrode. In addition, an almost constant ESR of 8.7 Ω during the first charge suggests forming a stable SEI layer. Additionally, the decrease of EDR from 308 Ω to 123 Ω during the first discharge process in Fig. 3b further confirms the SEI formation. Overall, EIS is a valuable method for determining D_{Na+}, and these data will be used to compare with values obtained from the GITT and PITT.

3.5. Comparison of D_{Na+} determined by GITT, EIS, and PITT

D_{Na+} values of tin phosphide electrodes estimated by GITT, EIS, and PITT techniques are compared in Fig. 4 and Table 1. Irrespective of the method used, the relationship between the D_{Na+} and the potential remains unchanged. D_{Na+} from PITT are similar to the values measured from GITT, in good agreement, meaning that the two methods are complementary. D_{Na+} values obtained from PITT during discharge are 3.67×10^{-10} cm^2 s^{-1} except for potential below 0.5 V vs. Na/Na^+. However, D_{Na+} from EIS during discharge is more widely distributed than the values from GITT and PITT. During the charging process, when the insertion potential is greater than 0.6 V vs. Na/Na^+, D_{Na+} values determined from EIS deviate from the GITT and PITT values. For the EIS, the medium frequency Warburg contribution of the impedance response is directly related to the sodium-ion diffusion process in Sn_4P_3 [16]. Besides, the equation for D_{Na+} from the impedance response is based on Fick's diffusion first law and Butler–Volmer equation [8]. Moreover, D_{Na+} of GITT and PITT in the electrode obeys Fick's second law [7,9]. Calculation of Impedance considers the impact of internal resistance, while GITT and PITT methods eliminate the impact of internal resistance [8]. These reasons lead to the D_{Na+} values obtained from EIS during discharge being more broadly dispersed than those obtained from GITT and PITT. Among the three methods of GITT, PITT, and EIS, GITT is simple to use, and values can be calculated easily. At the same time, PITT is complex in the experimental setup but simple in the calculation.

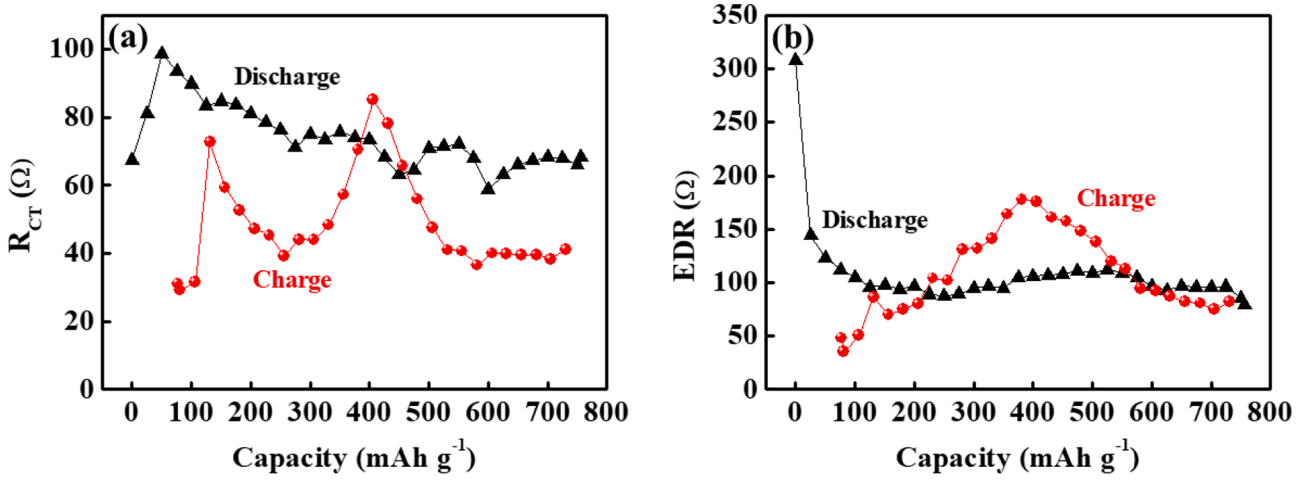

Fig. 3. (a) R_{CT} and (b) EDR of tin phosphide electrode with a thickness of 30 μm during EIS measurements.

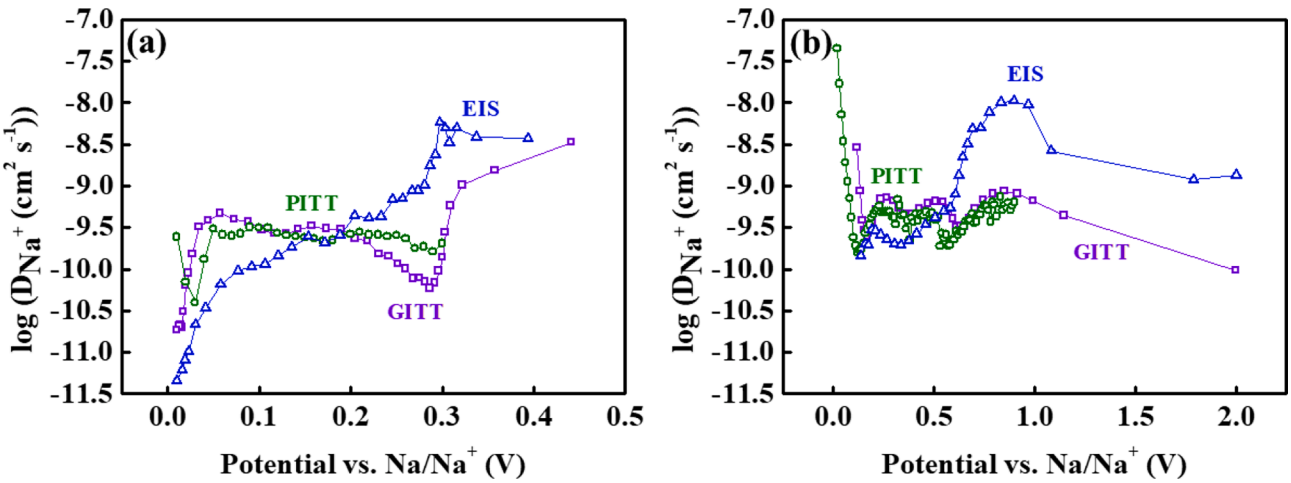

Fig. 4. D_{Na+} computed from the first (a) discharge and (b) charge GITT, PITT, and EIS curves for tin phosphide electrodes with a thickness of 30 μm at 50 mA g^{-1}.

Table 1
D_{Na+} calculated from the first discharge/charge GITT, PITT, and EIS curves for tin phosphide electrodes with a thickness of 30 μm at 50 mA g^{-1}. The unit for all diffusion coefficients is cm^2 s^{-1}.

	GITT	PITT	EIS
discharge	1.84×10^{-11} to 3.34×10^{-9}	3.93×10^{-11} to 3.67×10^{-10}	4.55×10^{-12} to 5.77×10^{-9}
Charge	9.57×10^{-11} to 2.88×10^{-9}	3.93×10^{-11} to 1.91×10^{-10}	1.44×10^{-10} to 1.05×10^{-8}

Although EIS can obtain information regarding ion dynamics, the data analysis on this method is quite laborious. According to the first principle theoretical calculation [17], the value of D_{Na+} in Sn_4P_3 has been found in the range of 3×10^{-8} to 10^{-7} (Table 2). However, comparable D_{Na+} values in our work (without additive) to those determined in ref 14–16 prove that enhanced Na-ion diffusion can be achieved with better electrode preparation, such as ball-milling of Sn_4P_3.

4. Conclusions

GITT, PITT, and EIS techniques were used to calculate the sodium-ion diffusion coefficients in tin phosphide. These methods are complementary in evaluating the kinetic barrier of sodium insertion/de-insertion in tin phosphide. In addition, valuable information regarding the state of electrode material and the effects of SEI on sodium insertion/de-insertion can be obtained in this way. These results suggest that electrode thickness strongly influences sodium transport in the bulk electrode and could impact the overall performance of the sodium-ion battery or capacitor. To achieve high capacity and cyclability of tin phosphide, electrode thickness should be as low as possible, as increasing thickness results in potential hysteresis. Since the fast charging might cause phase changes and result in the deterioration of electrode material, it is recommended to perform initial sodium insertion at low applied currents to fully access the bulk tin phosphide. Comparable values of D_{Na+} obtained with GITT, PITT, and EIS measurements suggest these electrochemical methods are prospective and complementary for determining the diffusion coefficients. Nevertheless, GITT is more suitable for evaluating D_{Na+} in tin phosphide due to its ease of experimental setup and data analysis.

CRediT authorship contribution statement

Jun Wang: Software, Writing – original draft, Investigation, Funding acquisition. **Emmanuel Pameté:** Methodology, Validation, Visualization, Writing – review & editing. **Shengli Yan:** Writing – review & editing, Resources. **Wenhua Zhao:** Resources, Writing – review & editing. **Jianhui Zhang:** Funding acquisition, Validation, Writing – review & editing. **Xiaotong He:** Writing – review & editing. **Zhazira Supiyeva:** Validation, Writing – review & editing. **Qamar Abbas:** Investigation, Supervision, Validation, Visualization, Writing – review & editing. **Xuexue Pan:** Resources, Data curation, Conceptualization, Writing – review & editing.

Table 2
Comparison of D_{Na+} from the literature and this work.

Material	Method	Electrolyte	D^+_{Na} (cm^2 s^{-1})	Material preparation	Reference
Sn_4P_3	first-principles molecular dynamics simulations	None	3×10^{-8} to 10^{-7}	None	[17]
Sn_4P_3@CNT/C	EIS	1 M $NaPF_6$ in DME	6.6×10^{-11} to 1.5×10^{-9}	Hydrothermal, carbon coating, phosphorization	[13]
Sn_4P_3@CN	GITT	1 M $NaClO_4$ in EC/DEC (vol. ratio 1:1) with 5 mass% FEC	10^{-14} to 10^{-15}	precipitate, heat reduction, phosphating	[14]
Sn_4P_3/C	GITT	1 M $NaPF_6$ in EC-DMC-FEC (vol. ratio 4.5/4.5/1)	$0.2–2.0 \times 10^{-12}$	Ball milling	[15]
Sn_4P_3	GITT	1 M $NaClO_4$ in EC/PC (volume ratio 1:1)	1.8×10^{-11} to 3.3×10^{-9}	Ball milling	This work

Declaration of Competing Interest

The authors declare that they have no known competing financial interests or personal relationships that could have appeared to influence the work reported in this paper.

Data availability

The data that has been used is confidential.

Acknowledgments

The authors are grateful to the Special Project in Key Fields of General Universities in Guangdong Province (No. 2022ZDZX3086), High-level Talents Research Initiative Project of Zhongshan City (No. KYG2101, KYG2202, and KYG2302), Characteristic Innovation Project of Ordinary Colleges and Universities in Guangdong Province (No. 2022KTSCX339). X.P. thanks the HYCAP project (research grant TEAM TECH/POIR.04.04.00-00-3D6F/16-00) funded by the Foundation for Polish Sciences (FNP). Q.A thanks The Austrian Research Promotion Agency (FFG) Austria for providing funds for the project number 39966764. E.P. acknowledges the financial support from the Alexander von Humboldt Foundation. Authors are grateful to Volker Presser (INM) for his suggestions to improve the manuscript.

Appendix A. Supplementary material

Supplementary data to this article can be found online at https://doi.org/10.1016/j.elecom.2023.107488.

References

[1] M.A. Rahman, J.H. Kim, S. Hossain, Recent advances of energy storage technologies for grid: A comprehensive review, Energy Storage (2022) e322, https://doi.org/10.1002/est2.322.
[2] J.J. Lamb, O.S. Burheim, Lithium-Ion Capacitors: A Review of Design and Active Materials, Energies 14 (2021) 979, https://doi.org/10.3390/en14040979.
[3] M.L. Divya, Y.-S. Lee, V. Aravindan, Solvent co-intercalation: an emerging mechanism in Li-, Na-, and K-ion capacitors, ACS Energy Lett. 6 (2021) 4228–4244, https://doi.org/10.1021/acsenergylett.1c01801.
[4] K. Turcheniuk, D. Bondarev, G.G. Amatucci, G. Yushin, Battery materials for low-cost electric transportation, Mater. Today 42 (2021) 57–72, https://doi.org/10.1016/j.mattod.2020.09.027.
[5] F. Duffner, N. Kronemeyer, J. Tübke, J. Leker, M. Winter, R. Schmuch, Post-lithium-ion battery cell production and its compatibility with lithium-ion cell production infrastructure, Nat. Energy 6 (2021) 123–134, https://doi.org/10.1038/s41560-020-00748-8.
[6] W. Zhao, X. Ma, L. Gao, Y. Li, G. Wang, Q. Sun, Engineering carbon-nanochain concatenated hollow Sn_4P_3 nanospheres architectures as ultrastable and high-rate anode materials for sodium ion batteries, Carbon 167 (2020) 736–745, https://doi.org/10.1016/j.carbon.2020.06.050.
[7] K. Tang, X. Yu, J. Sun, H. Li, X. Huang, Kinetic analysis on $LiFePO_4$ thin films by CV, GITT, and EIS, Electrochim. Acta 56 (2011) 4869–4875, https://doi.org/10.1016/j.electacta.2011.02.119.
[8] Y. Bai, X. Wang, X. Zhang, H. Shu, X. Yang, B. Hu, Q. Wei, H. Wu, Y. Song, The kinetics of Li-ion deintercalation in the Li-rich layered $Li_{1.12}[Ni_{0.5}Co_{0.2}Mn_{0.3}]_{0.89}O_2$ studied by electrochemical impedance spectroscopy and galvanostatic intermittent titration technique, Electrochim. Acta 109 (2013) 355–364, https://doi.org/10.1016/j.electacta.2013.06.134.
[9] J. Li, F. Yang, X. Xiao, M.W. Verbrugge, Y.-T. Cheng, Potentiostatic intermittent titration technique (PITT) for spherical particles with finite interfacial kinetics, Electrochim. Acta 75 (2012) 56–61, https://doi.org/10.1016/j.electacta.2012.04.050.
[10] J. Fang, W. Shen, S.H.S. Cheng, S. Ghashghaie, H.K. Shahzad, C. Chung, Four-electrode symmetric setup for electrochemical impedance spectroscopy study of Lithium-Sulfur batteries, J. Power Sources 441 (2019), 227202, https://doi.org/10.1016/j.jpowsour.2019.227202.
[11] D.V. Horváth, J. Coelho, R. Tian, V. Nicolosi, J.N. Coleman, Quantifying the dependence of battery rate performance on electrode thickness, ACS Appl. Energy Mater. 3 (10) (2020) 10154–10163, https://doi.org/10.1021/acsaem.0c01865.
[12] Y. Xu, Z. Lin, X. Zhong, X. Huang, N.O. Weiss, Y. Huang, X. Duan, Holey graphene frameworks for highly efficient capacitive energy storage, Nat. Commun. 5 (2014) 4554, https://doi.org/10.1038/ncomms5554.
[13] L. Ran, B. Luo, I.R. Gentle, T. Lin, Q. Sun, M. Li, M.M. Rana, L. Wang, R. Knibbe, Biomimetic Sn_4P_3 anchored on carbon nanotubes as an anode for high-performance sodium-ion batteries, ACS Nano 14 (2020) 8826–8837, https://doi.org/10.1021/acsnano.0c03432.
[14] T. Zeng, D. Feng, Y. Xie, X. Jiao, Nano Sn_4P_3 embedded in nitrogenous carbon matrix as the anode of sodium ion battery for enhanced cyclability, J. Alloys Compd. 874 (2021), 159944, https://doi.org/10.1016/j.jallcom.2021.159944.
[15] J. Zhou, X. Lian, Y. You, Q. Shi, Y.u. Liu, X. Yang, L. Liu, D. Wang, J.-H. Choi, J. Sun, R. Yang, M.H. Rummeli, Revealing the various electrochemical behaviors of Sn_4P_3 binary alloy anodes in alkali metal ion batteries, Adv. Funct. Mater. 31 (31) (2021) 2102047, https://doi.org/10.1002/adfm.202102047.
[16] M. Reddy, R. Jose, A. Le Viet, K.I. Ozoemena, B. Chowdari, S. Ramakrishna, Studies on the lithium ion diffusion coefficients of electrospun Nb_2O_5 nanostructures using galvanostatic intermittent titration and electrochemical impedance spectroscopy, Electrochim. Acta 128 (2014) 198–202, https://doi.org/10.1016/j.electacta.2013.10.003.
[17] S.C. Jung, J.-H. Choi, Y.-K. Han, The origin of excellent rate and cycle performance of Sn_4P_3 binary electrodes for sodium-ion batteries, J. Mater. Chem. A 6 (2018) 1772–1779, https://doi.org/10.1039/C7TA07310K.